

Determination of the Solubility Limit of Tris(dibenzylideneacetone) dipalladium(0) in Tetrahydrofuran/Water Mixtures

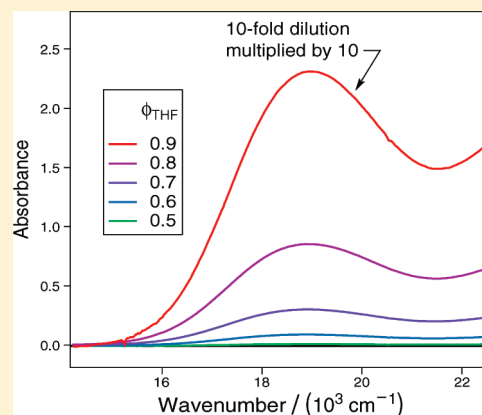
Stefan Franzen*

Department of Chemistry, North Carolina State University, Raleigh, North Carolina 27695, United States

S Supporting Information

ABSTRACT: Determination of the solubility limit of a strongly colored organometallic reagent in a mixed-solvent system provides an example of quantitative solubility measurement appropriate to understand polymer, nanoparticle, and other macromolecular aggregation processes. The specific example chosen involves a solution of tris(dibenzylideneacetone) dipalladium(0), $\text{Pd}_2(\text{dba})_3$, in THF/ H_2O mixtures, which has the desired properties of high absorption in the visible range ($\lambda_{\text{max}} = 528 \text{ nm}$) and significant difference in solubility in the two solvents THF and H_2O . $\text{Pd}_2(\text{dba})_3$ is readily available, safe, and commonly used in nanoparticle syntheses. The application of Flory–Huggins theory permits the fit of a quantitative model to data obtained from a straightforward laboratory experiment that can be conducted in less than 3 h. The absorbance of this compound is easily measured by UV–vis absorption spectroscopy. The application of the Beer–Lambert law to the data in this experiment is a useful exercise for students because the absorbances span three orders of magnitude.

KEYWORDS: Upper-Division Undergraduate, Laboratory Instruction, Physical Chemistry, Hands-On Learning/Manipulatives, Computer-Based Learning, Solutions/Solvents, Thermodynamics, Nanotechnology, Colloids, UV-Vis Spectroscopy



The study of molecular solubility and the study of solvent mixtures are both classic problems in physical chemistry taught to undergraduate students. However, the solubility of solutes in mixed organic–aqueous solution is not commonly discussed, although it has increasing application in the synthesis of nanoparticles, polymer synthesis, metal extraction, and crystallization. Control of aggregation by means of the solvent conditions is important in the growing field of nanoparticle synthesis.^{1–11} The solubility of organic molecules relevant to polymer synthesis has been considered most often in the context of Flory–Huggins theory.^{12,13} The application of theory to the solubility of organic molecules differs from that of ions, which has been considered in detail owing to the many practical applications, such as extraction of metals from ore.¹⁴ The increase in metal ion solubility in solvent mixtures arises largely from specific coordination by solvents (e.g., acetonitrile coordinating Ag^+).^{15,16} Counter ion effects have also been considered, as well as exceptions to solubility rules.¹⁷ Crystallization, on the other hand, involves balancing solubility at the point where controlled growth competes effectively with aggregation. This can be done by introducing a second solvent to reduce the solubility.^{18,19} The solvent with poor ability to dissolve the solute is known as the nonsolvent. Because of the need to train scientists to understand the technological significance, there are numerous recent examples of laboratory demonstrations for understanding solubility in complex systems.^{20–22} The experiment described in this

article is aimed at understanding this phenomenon and related solubility rules.

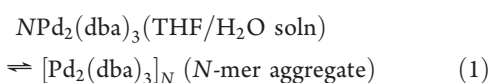
We have chosen a material that is known to form both nano- and microcrystals in solution, the organometallic reagent tris(dibenzylideneacetone) dipalladium(0), $\text{Pd}_2(\text{dba})_3$.^{5,7,8,23–25} Although we will not explore the aspect of Pd nanoparticle synthesis using $\text{Pd}_2(\text{dba})_3$ in this laboratory example, there are examples of nanoparticle formation in a reducing environment (i.e., in the presence of CO or H_2 gas).²⁶ The precipitate that is discarded in this exercise contains many nanoparticles, which are similar in structure^{23–25} to those studied elsewhere.^{5,7,8} $\text{Pd}_2(\text{dba})_3$ is best known as a means of delivering active Pd in solution for homogeneous catalysis of bond-forming reactions such as the Heck reaction, Sonogashira coupling, Negishi coupling, Carroll rearrangement, and Trost asymmetric allylic alkylation.^{27–29} However, metallic Pd is formed by allylic and phosphine groups in organic solvents and not by the THF/ H_2O mixture, which is relatively inert. The precipitate contains many crystals of $\text{Pd}_2(\text{dba})_3$, formed by the lack of solubility in the THF/ H_2O mixtures, whereas Pd nanoparticles are a minority species under these conditions.^{23–25}

The nature of mixed-solvent organic–aqueous solutions provides an excellent visual example of the effect of differential

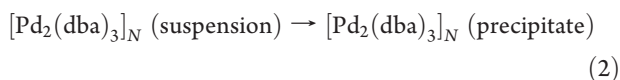
solubility. $\text{Pd}_2(\text{dba})_3$ is a strongly colored organometallic molecule that shows a wide range of solubility in THF/ H_2O mixtures, ranging from soluble in pure THF to virtually insoluble in pure H_2O . Thus, THF and H_2O are the solvent and nonsolvent, respectively, in this system. In the experiment described here, the solubility of an organometallic molecule in a mixed-solvent system illustrates solubility in mixed solvents as it applies to aggregation and crystallization. The solubility properties of organometallic $\text{Pd}_2(\text{dba})_3$ are applicable to a wide range of organic molecules that lack the conveniently observable UV–vis absorption band. The solutions that can be easily prepared in this exercise permit direct observation of rapid aggregation leading to precipitation, on the one hand, and slow aggregation leading to crystal formation, on the other. Finally, because THF/ H_2O solutions are somewhat unstable and tend to lose $\text{Pd}(0)$ to form spherical nanoparticles, there is interesting behavior in the formation of precipitates or mixtures of crystals. These can be observed readily under a light microscope. Consequently, $\text{Pd}_2(\text{dba})_3$ in THF/ H_2O mixtures provide an excellent example relevant to particle formation, which can be incorporated into the observations recorded in the laboratory experiment. Such a simple system that exemplifies all of these aspects of the important role played by the nonsolvent has practical benefit for training students. The THF/ H_2O two-component mixture is widely studied as an example of a “closed-loop” system, which has both an upper and lower critical point such that the two-phase region is completely surrounded by single-phase region.³⁰ The critical point is above 70 °C in THF/ H_2O at 1 atm of pressure so that the complication of the critical behavior can be avoided in the laboratory exercise. The laboratory example is a much-needed study of organic solubility that complements the more commonly studied ionic solubility.

THEORY

The theory of solubility of organic compounds in two-component mixtures is related to the theory of aggregation, which branches into the theory of micelle formation,³¹ polymer formation, and crystallization. One can write the equilibrium as



where N is the stoichiometric coefficient and the associated aggregation Gibbs energy is $\Delta_{\text{ag}}G_N$. The aggregate may remain in a suspension or may precipitate. The suspendability is given by



The suspendability of the $[\text{Pd}_2(\text{dba})_3]_N$ aggregate is not governed by an equilibrium constant as the aggregate is intrinsically unstable with respect to solidification. Thus, there is an important distinction that should be made between a solution and a suspension. This is extremely relevant in the chemical literature today given the number of nanoparticle syntheses that cross the boundary from a solution to a suspension as part of the protocol for synthesis.

The rules of colloid chemistry determine the time scale on which aggregates will remain suspended. Derjaguin–Landau–Verwey–Overbeek (DLVO) theory, the theory of colloidal stability, is based on the role of charge stabilization as a balance

to ubiquitous van der Waals forces that lead to flocculation and aggregation.³² Since $[\text{Pd}_2(\text{dba})_3]_N$ is a neutral aggregate, there is only a van der Waals force without a balancing electrostatic repulsion term and rapid precipitation is expected.³³ Visual observation confirms that precipitation is rapid in this system. The aggregation equilibrium provides an intuitive picture of formation of a “nanoparticle” that is no longer soluble and hence precipitates, but the theory of mixed solvents is complicated in this case. On the other hand, the theory of solubility in mixed solvents provides a quantitative explanation that relates to the solubility in the pure solvents, without explicitly mentioning how the solute is destabilized. Hence, Flory–Huggins and aggregation equilibrium–DLVO theory provide two complementary views to the Gibbs energy that governs solubility.

THE AGGREGATION EQUILIBRIUM

The fact that $\text{Pd}_2(\text{dba})_3$ forms organic crystals, as observed by transmission electron microscopy (TEM) and light microscopy,²⁴ makes this system a test system for exploring the factors that govern the aggregation equilibria and solution stability in mixed solvents. Thus, $\text{Pd}_2(\text{dba})_3$ in THF/ H_2O solutions provides a range of solution behaviors with which to test solubility, suspendability, and crystal formation in the laboratory. The thermodynamics of aggregation due to the hydrophobic effect can be expressed in terms of an equilibrium constant for N -mer aggregate formation.³⁴ It is understood that this aggregate, once formed, is metastable according to DLVO theory. Thus, we expect that on some time scale precipitation will occur. First, we will derive the aggregation equilibrium and then we will show a complementary view based on Flory–Huggins theory.

The chemical potential of the solute, μ_1 , and the N -mer aggregate, μ_N , with activities a_1 and a_N , respectively, in a two component mixture can be written as

$$\mu_1 = \mu_1^\circ + k_B T \ln a_1 \quad (3)$$

$$\mu_N = \mu_N^\circ + k_B T \ln a_N \quad (4)$$

where k_B is the Boltzmann constant and T is the absolute temperature. The Gibbs energy change for the reaction, eq 1, is

$$\Delta_{\text{ag}}G_N = \mu_N - N\mu_1 \quad (5)$$

At equilibrium $\Delta_{\text{ag}}G_N = 0$, and we can write

$$\mu_N^\circ + k_B T \ln a_N = N(\mu_1^\circ + k_B T \ln a_1) \quad (6)$$

If we define $\Delta_{\text{ag}}G_N^\circ = \mu_N^\circ - N\mu_1^\circ$, then the expression becomes

$$\ln a_1 = [(\ln a_N)/N] + [\Delta_{\text{ag}}G_N^\circ / (Nk_B T)] \quad (7)$$

which determines the extents of aggregation of N -mers in equilibrium with monomers. Technically speaking, the aggregate is in a suspension and not a solution. If the aggregate is sufficiently large or colloidal unstable, it will precipitate. Because N -mer is removed from suspension, the equilibrium in eq 1 is shifted toward the right. At some point the solubility limit is reached and no further precipitation occurs. At this point, we can consider the system a solution, rather than a suspension. We define the solubility limit as the maximum concentration of the monomer solute for which a solution occurs.

The $\text{Pd}_2(\text{dba})_3$ unit cell is approximately $1.3 \times 1.3 \times 1.5 \text{ nm}^3$ or 2.5 nm^3 .^{3,35} In pure THF, a typical size for a hexagonal aggregate of $\text{Pd}_2(\text{dba})_3$ is 500 nm in diameter, in 50% THF/50%

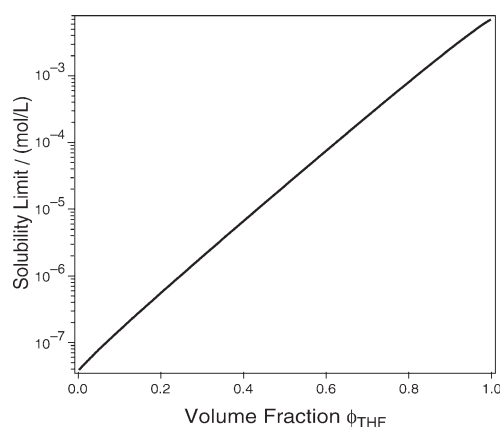


Figure 1. Calculated solubility limit based on Flory–Huggins theory. The solubility limit was calculated using eq 8 with values of $\Delta_{\text{sol}}G_{\text{THF}}^{\circ} = 12.2$ kJ/mol, $\Delta_{\text{sol}}G_{\text{W}}^{\circ} = 42.5$ kJ/mol, and $\chi_{\text{W,THF}} = 1.5$, as described in the text.

H_2O ,^{5,7,8,23–25} giving a volume of $2 \times 10^7 \text{ nm}^3$ composed of $\sim 10^7$ monomers. Because $\text{Pd}_2(\text{dba})_3$ is virtually insoluble in pure H_2O ,³⁶ it is difficult to assess the magnitude of N in that solvent. However, we have observed a decrease in aggregate size as the solvent hydrophobicity increases, which may be a result of the greater solubility of the monomer. The decrease in aggregation size is analogous to the disappearance of a well-defined micelle for surfactants in nonaqueous solvents.³⁷ The aggregation and colloidal instability of $\text{Pd}_2(\text{dba})_3$ in THF/ H_2O solutions appears to be comparable to the stability of polymers in solvent mixtures. These considerations justify the use of Flory–Huggins theory to model the solubility limit of $\text{Pd}_2(\text{dba})_3$ in equilibrium with its aggregates.

■ SOLUBILITY OF SOLUTES IN MIXED-SOLVENT SYSTEMS: FLORY–HUGGINS THEORY

$\text{Pd}_2(\text{dba})_3$ monomer is observed to be soluble only in the THF fraction, and hence, $\text{Pd}_2(\text{dba})_3$ aggregates will tend to precipitate as the volume fraction of H_2O increases in a mixed-solvent system. Starting with the standard Gibbs energies of solvation of $\text{Pd}_2(\text{dba})_3$ in pure H_2O and THF, which are $\Delta_{\text{sol}}G_{\text{W}}^{\circ}$ and $\Delta_{\text{sol}}G_{\text{THF}}^{\circ}$, respectively, the Gibbs energy for solution in the mixture, $\Delta_{\text{sol}}G_{\text{mix}}^{\circ}$, can be expressed using Flory–Huggins theory

$$\Delta_{\text{sol}}G_{\text{mix}}^{\circ}/(RT) = \phi_{\text{W}}\Delta_{\text{sol}}G_{\text{W}}^{\circ}/(RT) + \phi_{\text{THF}}\Delta_{\text{sol}}G_{\text{THF}}^{\circ}/(RT) + \phi_{\text{W}} \ln \phi_{\text{W}} + \phi_{\text{THF}} \ln \phi_{\text{THF}} + \chi_{\text{W,THF}}\phi_{\text{W}}\phi_{\text{THF}} \quad (8)$$

where $\phi_{\text{W}} = V_{\text{W}}/V$ and $\phi_{\text{THF}} = V_{\text{THF}}/V$ are the volume fractions of water and THF, respectively, and $\chi_{\text{W,THF}}$ is the Flory–Huggins interaction parameter for THF and H_2O .^{12,38–40} By knowing the solubility in THF, we can calculate

$$\ln a_1 = -\Delta_{\text{sol}}G_{\text{mix}}^{\circ}/(RT) \quad (9)$$

in the mixed-solvent system. Given estimates of $\Delta_{\text{sol}}G_{\text{THF}}^{\circ} = 12.2$ kJ/mol and $\Delta_{\text{sol}}G_{\text{W}}^{\circ} = 42.5$ kJ/mol, based on the experiment shown below, combined with an estimate of 1.5 for the Flory–Huggins parameter of a THF/ H_2O mixture, we can calculate the theoretical solubility plot in Figure 1. The plot of

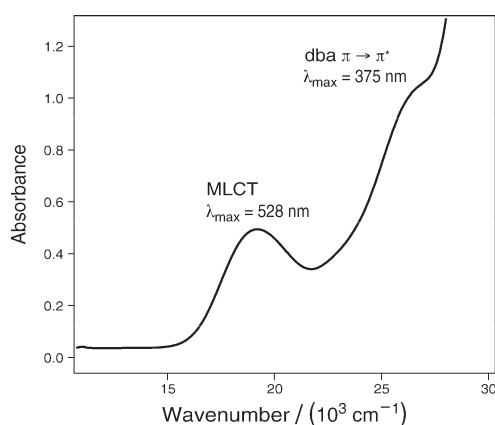


Figure 2. Absorption spectrum of a 500 μM solution of $\text{Pd}_2(\text{dba})_3$ in THF. The metal-to-ligand charge transfer band at 528 nm is labeled MLCT in the figure. The dba ligand transition is an aromatic $\pi \rightarrow \pi^*$ transition at 375 nm.

solubility is linear on a semi-log plot in accord with eq 9, which makes a simple presentation for the student.

■ EXPERIMENTAL PROCEDURE

For measurements of the solubility limit, 73.2 mg of tris(dibenzylideneacetone dipalladium(0), $\text{Pd}_2(\text{dba})_3$ (STREM catalog no. 51364-51-3, $M_r = 915.7$), was dissolved in 20 mL of anhydrous tetrahydrofuran (THF) to make a 4 mM stock solution. When employed as a catalyst, $\text{Pd}_2(\text{dba})_3$ is often weighed and dissolved in a glove box. However, for the present experiment, $\text{Pd}_2(\text{dba})_3$ will be mixed immediately with H_2O and exposed to air, so that a glove box is not necessary. The resulting solution had a deep purple color. Solutions of varying percentage of THF and H_2O were prepared by quickly pipetting an appropriate volume of the 4 mM stock solution of $\text{Pd}_2(\text{dba})_3$ in THF into vials containing H_2O to make THF/ H_2O mixtures ranging from 90% THF to 10% THF with total volume of 2 mL. The nominal $\text{Pd}_2(\text{dba})_3$ concentration obtained was equal to $(\text{THF}\%/100) \times 4 \text{ mM}$. For example, a 10% THF/90% H_2O solution would correspond to 400 μM $\text{Pd}_2(\text{dba})_3$ and a 90% THF/10% H_2O solution would correspond to 3.60 mM $\text{Pd}_2(\text{dba})_3$, if $\text{Pd}_2(\text{dba})_3$ were completely soluble. However, a precipitate was immediately observed in all solutions studied. Therefore, the mixtures were immediately centrifuged at 10,000 rpm for 5 min, the precipitate was removed, and the supernatant containing a saturated solution of $\text{Pd}_2(\text{dba})_3$ was used for the solubility measurements. Filtration of the precipitates through a Whatman 0.02 μm filter gives results that are similar to those obtained by centrifugation.

Absorption spectra of the supernatant from the centrifuged solutions were measured using a HP8542 photodiode array spectrophotometer. Measurements under a variety of conditions showed that exposure to oxygen for periods of many hours or even days did not affect the spectra.

To convert the absorbance measurements to concentration using the Beer–Lambert law, the extinction coefficient, ϵ , of the 528 nm ($18,940 \text{ cm}^{-1}$) metal-to-ligand charge transfer (MLCT) absorption band of $\text{Pd}_2(\text{dba})_3$ shown in Figure 2 was determined to be $8,970 \text{ L mol}^{-1} \text{ cm}^{-1}$ by repeated measurements of the absorbance using quantities of $\text{Pd}_2(\text{dba})_3$ ranging from 4.6 to 70.3 mg dissolved in 20 mL of THF solution and assuming complete dissolution of $\text{Pd}_2(\text{dba})_3$. This value is significantly

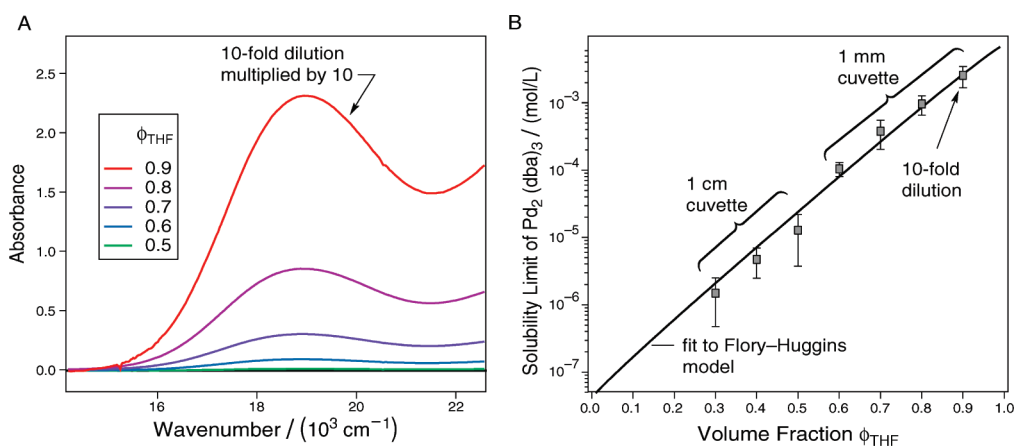


Figure 3. (A) Absorbance data for mixtures made by addition of 4 mM $\text{Pd}_2(\text{dba})_3$ in dry THF solutions to H_2O . The 90% THF sample was multiplied by a factor of 10 because a diluted sample was used for the actual measurement to avoid measuring an absorbance $A_{528\text{ nm}} > 1$. (B) Solubility of $\text{Pd}_2(\text{dba})_3$ in THF. Concentrated solutions are purple in color and a 1 mm cuvette was required above 60% THF. The sample at a volume fraction of 90% THF was too concentrated to measure accurately in a 1 mm cuvette so it was diluted by a factor of 10 prior to measurement as indicated. Below 30% THF, suspensions of $\text{Pd}_2(\text{dba})_3$ are transparent and lack any color.

lower than the value of $19,500\text{ L mol}^{-1}\text{ cm}^{-1}$ measured previously by Gray and co-workers in pure 2-methyl THF,⁴¹ which may be due to the tendency of $\text{Pd}_2(\text{dba})_3$ to spontaneously form aggregates even in pure THF.²⁴ All of the solutions had a measurable absorption at $26,670\text{ cm}^{-1}$ (375 nm) due to the $\pi \rightarrow \pi^*$ transition of free dba. As observed in Figure 2, this band did not interfere with the solubility measurements based on the MLCT band.

The optimum method for measurement of solubility would involve the use of a variable path length cell. Because such cells are usually not available, the recommended procedure uses a combination of standard 1 mm and 1 cm path length cells to span an absorbance range of the saturated solutions from $A \sim 0.001$ in 30% THF solutions (1 cm path length) to $A > 20$ in a 1 cm path length equivalent. Owing its high absorbance, the 90% THF concentration was diluted by a factor 10, and then the absorbance was measured in a 1 mm cuvette (Figure 3A). Below 30% THF, the absorbance was too low to obtain a measurement in a 1 cm path length cell ($A < 0.001$), which is the longest convenient path length in the HP8542 spectrophotometer (Figure 3A).

HAZARDS

Tris(dibenzylideneacetone) dipalladium(0) or $\text{Pd}_2(\text{dba})_3$ may irritate the eyes, skin, and the digestive tract. The toxicological properties of this substance have not been fully investigated. Tetrahydrofuran is volatile, highly flammable, and may contain peroxides. Peroxides are explosive. They are easily formed from tetrahydrofuran and air on ambient light and may accumulate up to dangerous concentration when tetrahydrofuran dries out.

RESULTS

The solutions prepared by centrifugation or filtering are stable for a period days or weeks. Because excess $\text{Pd}_2(\text{dba})_3$ is used for all solvent mixtures, saturation will be observed by precipitation. Figure 3A shows the observed UV–vis absorption spectra of the supernatant following centrifugation at 10,000 rpm for 5 min to remove the $\text{Pd}_2(\text{dba})_3$ precipitate. Figure 3B shows the averaged data obtained from a measurement of the absorbance at 528 nm divided by the extinction coefficient and path length to convert to

concentration. The errors were obtained as the standard deviation of three replicate measurements. The fit function was programmed into IgorPro 5.0 (see the Supporting Information). The two adjustable parameters are $\Delta_{\text{sol}}G_{\text{W}}^\circ$ and $\Delta_{\text{sol}}G_{\text{THF}}^\circ$.

DISCUSSION

The essentially complete lack of solubility of $\text{Pd}_2(\text{dba})_3$ in water combined with its pronounced visible absorption bands provide a useful way to measure the solubility limit in mixed-solvent systems. We have chosen the system THF and water because the solvents are completely miscible below the critical point of $\sim 70^\circ\text{C}$ at 1 atm. Measurements of this type provide students with a fundamental understanding of how the solubility limit can be determined, but more importantly, it is the starting point for understanding aggregation equilibria that can lead to formation of nanostructures in solution. At a time when nanoparticle synthesis is occupying a growing part of the chemical literature, this approach has a great deal of relevance.

The laboratory exercise should be combined with a description of the errors and sources of random, as well as systematic, error. Random error in this case is associated with measurement error that arises from the variability in concentration due to errors in weighing or mixing. The error associated with the absorbance measurement is relatively small. For practical reasons, it may not be possible to make three independent measurements in the same class period. However, one possible way to approach the random error is to have teams of students make the measurement in parallel and combine their data to observe the measurement error. The systematic error in this experiment arises from possible effects owing to differences in aggregation conditions. Aggregates of $\text{Pd}_2(\text{dba})_3$ tend to form spontaneously even after centrifugation or filtering. The students may be able to observe this by a second round of centrifugation to observe a small quantity of precipitate even after the first pass. This relatively small error can be included in the analysis.

The measurement spans a wide range of absorbance. The instructor may wish to review the Beer–Lambert law, $A = \epsilon cd$ where ϵ is the extinction coefficient ($\text{L mol}^{-1}\text{ cm}^{-1}$), c is the concentration in molarity (M), and d is the path length (in cm).

Students should be cautioned that accurate measurement requires $A_{528\text{ nm}} < 1$ for greatest accuracy. Students will need to examine their measurement to see if $A_{528\text{ nm}}$ exceeds 1 for a given solution. In that case, the students may need to make an appropriate dilution to obtain an accurate measurement. They may need to be reminded of the dilution factor equation $C_1V_1 = C_2V_2$, where C_i and V_i are the concentration and volume of sample i , respectively. Since the transmitted intensity depends on 10^{-A} , the quantity of light reaching the detector drops below 10%, when $A > 1$. Although it is somewhat arbitrary, there is clearly a point at which the signal-to-noise ratio suffers from low light intensity. Because the concentration depends exponentially on the solvent volume fraction according to Flory–Huggins theory, the concentrations, and therefore absorbances of the samples at 528 nm, span more than 3 orders of magnitude in this experiment. The most concentrated solutions have $A_{528\text{ nm}} > 2$ even in a 1 mm cuvette. Thus, students will need to reason how to measure absorbance in such concentration solutions. The data in Figure 3 show that the solution was diluted by a factor of 10 at the highest THF volume fraction in order to make a measurement in the linear range.

Students can also compare their results to studies that have been carried out the chemical literature. $\text{Pd}_2(\text{dba})_3$ has been used as a precursor in nanoparticle synthesis in a number of studies. Clearly, the mixed-solvent solubility is of great interest in understanding the mechanism for such syntheses. To increase the student's awareness of the importance to read the chemical literature critically, students may wish to consult studies that use mixed solvents. One recent reference shows a picture of a solution of $400\text{ }\mu\text{M}$ $\text{Pd}_2(\text{dba})_3$ in 10%THF/90% H_2O .⁴² The data in Figure 3B show that these reported values⁴² are >3,000 times higher than the solubility limit. It would be instructive for students to compare this claim with their measurement and comment on this in the laboratory report.

CONCLUSION

The student laboratory experiment described here dispels a common misconception that solubility scales linearly with the solvent composition. In fact, the exponential dependence of chemical equilibrium, and therefore solubility in this case, on Gibbs energy is revealed by a colorimetric measurement of the concentration of a dye that is soluble in one solvent (THF), but insoluble in another (H_2O) in a two-component mixture. This fact can be demonstrated within about 2 h using inexpensive reagents and standard laboratory equipment; a weighing balance, UV–vis spectrophotometer (even single wavelength), a pipet, vials, and an optical cuvette.

ASSOCIATED CONTENT

Supporting Information

Student laboratory procedures; instructor notes. This material is available via the Internet at <http://pubs.acs.org>.

AUTHOR INFORMATION

Corresponding Author

*E-mail: Stefan_Franzen@ncsu.edu.

REFERENCES

- (1) Ramirez, E.; Jansat, S.; Philippot, K.; Lecante, P.; Gomez, M.; Masdeu-Bulto, A. M.; Chaudret, B. *J. Organomet. Chem.* **2004**, 689, 4601–4610.
- (2) Ren, J.; Tilley, R. D. *Small* **2007**, 3, 1508–1512.
- (3) Narayanan, R.; El-Sayed, M. A. *J. Catal.* **2005**, 234, 348–355.

- (4) Li, Y.; Boone, E.; El-Sayed, M. A. *Langmuir* **2002**, 18, 4921–4925.
- (5) Liu, D. G.; Gugliotti, L. A.; Wu, T.; Dolska, M.; Tkachenko, A. G.; Shipton, M. K.; Eaton, B. E.; Feldheim, D. L. *Langmuir* **2006**, 22, 5862–5866.
- (6) Green, M.; Smith-Boyle, D.; Harries, J.; Taylor, R. *Chem. Commun.* **2005**, 4830–4832.
- (7) Gugliotti, L. A.; Feldheim, D. L.; Eaton, B. E. *Science* **2004**, 304, 850–852.
- (8) Gugliotti, L. A.; Feldheim, D. L.; Eaton, B. E. *J. Am. Chem. Soc.* **2005**, 127, 17814–17818.
- (9) Kumar, A.; Kumar, V. *J. Phys. Chem. C* **2008**, 112, 3633–3640.
- (10) Xia, Y.; Xiong, Y. J.; Lim, B.; Skrabalak, S. E. *Angew. Chem., Intl. Ed.* **2009**, 48, 60–103.
- (11) Redjala, T.; Apostolecu, G.; Beaunier, P.; Mostafavi, M.; Etcheberry, A.; Uzio, D.; Thomazeau, C.; Remita, H. *New J. Chem.* **2008**, 32, 1403–1408.
- (12) Nagarajan, R.; Wang, C. C. *Langmuir* **2000**, 16, 5242–5251.
- (13) Bozdogan, A. E. *Polymer* **2003**, 44, 6427–6430.
- (14) Lorimer, J. W. *Pure Appl. Chem.* **1993**, 65, 183–191.
- (15) Tomkins, R. P. T. *J. Chem. Educ.* **2008**, 85, 310–316.
- (16) Subramanian, S.; Kalidas, C. *Electrochim. Acta* **1984**, 29, 753–756.
- (17) Blake, B. J. *Chem. Educ.* **2003**, 80, 1348–1350.
- (18) Ruckenstein, E.; Shulgin, I. L. *Adv. Colloid Interface Sci.* **2006**, 123, 97–103.
- (19) Woo, E. M.; Sun, Y. S.; Yang, C. P. *Prog. Polym. Sci.* **2001**, 26, 945–983.
- (20) Konrad, O.; Lankau, T. *J. Chem. Educ.* **2007**, 84, 864–869.
- (21) Passarelli, M. *J. Chem. Educ.* **2009**, 86, 845–846.
- (22) Katz, C. A.; Calzola, Z. J.; Mbindyo, J. K. N. *J. Chem. Educ.* **2008**, 85, 263–265.
- (23) Franzen, S.; Cerruti, M.; Leonard, D. N.; Duscher, G. *J. Am. Chem. Soc.* **2007**, 129, 15340–15346.
- (24) Leonard, D. N.; Cerruti, M.; Duscher, G.; Franzen, S. *Langmuir* **2008**, 24, 7803–7809.
- (25) Leonard, D. N.; Franzen, S. *J. Phys. Chem. C* **2009**, 113, 12706–12714.
- (26) Siril, P. F.; Ramos, L.; Beaunier, P.; Archirel, P.; Etcheberry, A.; Remita, H. *Chem. Mater.* **2009**, 21, 5170–5175.
- (27) Beller, M.; Fischer, H.; Kuhlwein, K.; Reisinger, C. P.; Herrmann, W. A. *J. Organomet. Chem.* **1996**, 520, 257–259.
- (28) Trost, B. M. *Tetrahedron* **1977**, 33, 2615–2649.
- (29) Trost, B. M.; Brieden, W.; Baringhaus, K. H. *Angew. Chem., Intl. Ed.* **1992**, 31, 1335–1336.
- (30) Vnuk, F. *J. Chem. Soc., Faraday Trans. 2* **1983**, 79, 57–64.
- (31) Nagarajan, R.; Ruckenstein, E. *Langmuir* **1991**, 7, 2934–2969.
- (32) Uskokovic, V. *Rev. Chem. Eng.* **2007**, 23, 301–372.
- (33) Verberg, R.; de Schepper, I. M.; Cohen, E. G. D. *Europhys. Lett.* **1999**, 48, 397–402.
- (34) Tanford, C. *The Hydrophobic Effect: Formation of Micelles and Biological Membranes*; Wiley-Interscience: New York, 1980.
- (35) Pierpont, C. G.; Mazza, M. C. *Inorg. Chem.* **1974**, 13, 1891–1895.
- (36) Rodman, D. L.; Carrington, N. A.; Xue, Z. L. *Talanta* **2006**, 70, 426–431.
- (37) Ruckenstein, E.; Nagarajan, R. *J. Phys. Chem.* **1980**, 84, 1349–1358.
- (38) Domanska, U.; Zolek-Tryznowska, Z. *J. Phys. Chem. B* **2009**, 113, 15312–15321.
- (39) Eser, H.; Tihminlioglu, F. *J. Appl. Polym. Sci.* **2006**, 102, 2426–2432.
- (40) Schild, H. G.; Muthukumar, M.; Tirrell, D. A. *Macromolecules* **1991**, 24, 948–952.
- (41) Harvey, P. D.; Adar, F.; Gray, H. B. *J. Am. Chem. Soc.* **1989**, 111, 1312–1315.
- (42) Gugliotti, L. A.; Feldheim, D. L.; Eaton, B. E. *J. Am. Chem. Soc.* **2009**, 131, 11634.